Empirical molecular-dynamics study of diffusion in liquid semiconductors

W. Yu
Photonic Materials and Devices Laboratory, Department of Materials Science and Physics, University of Southern California, Los Angeles, California 90089

Z. Q. Wang* and D. Stroud
Department of Physics, The Ohio State University, Columbus, Ohio 43210

(Received 11 July 1996)

We report the results of an extensive molecular-dynamics study of diffusion in liquid Si and Ge (ℓ-Si and ℓ-Ge) and of impurities in ℓ-Ge, using empirical Stillinger-Weber (SW) potentials with several choices of parameters. We use a numerical algorithm in which the three-body part of the SW potential is decomposed into products of two-body potentials, thereby permitting the study of large systems. One choice of SW parameters agrees very well with the observed ℓ-Ge structure factors. The diffusion coefficients $D(T)$ at melting are found to be approximately 6.4×10^{-5} cm^2/s for ℓ-Si, in good agreement with previous calculations, and about 4.2×10^{-5} and 4.6×10^{-5} cm^2/s for two models of ℓ-Ge. In all cases, $D(T)$ can be fitted to an activated temperature dependence, with activation energies E_d of about 0.42 eV for ℓ-Si, and 0.32 or 0.26 eV for two models of ℓ-Ge, as calculated from either the Einstein relation or from a Green-Kubo-type integration of the velocity autocorrelation function. $D(T)$ for Si impurities in ℓ-Ge is found to be very similar to the self-diffusion coefficient of ℓ-Ge. We briefly discuss possible reasons why the SW potentials give $D(T)$'s substantially lower than *ab initio* predictions. [S0163-1829(96)03644-2]

I. INTRODUCTION

The thermophysical properties of liquid semiconductors are of both practical and fundamental importance. On the practical side, most modern crystal growth methods, such as the Czochralski (CZ) process for growing single crystals of Si (c-Si), start from the liquid state. From the standpoint of pure science, the elemental semiconductors Si and Ge are actually metallic in the liquid state, yet they retain some traces of covalent bonding. This is most noticeable in the structure factors $S(k)$, which shows clear departures from the close packing typical of simple liquid metals such as Al and Na.

Among the thermophysical properties, the self-diffusion coefficients $D(T)$ of liquid semiconductors are of particular interest. These are needed as inputs to the fluid-dynamical equations which describe the crystal growth from the melt. Likewise, it is important to know the diffusion coefficients of impurities in semiconductors, in order to develop methods of purifying the resulting crystals. These diffusion coefficients are difficult to measure in the earth's gravitational field, because the resulting numbers are tainted by unavoidable convective processes. In addition, direct measurements of any thermophysical properties are quite difficult because of the elevated melting temperature and the high reactivity of most liquid semiconductors.[1–6] Thus theoretical studies are particularly needed for understanding these coefficients.

Because of recent advances in computational speed, many thermophysical properties of liquid semiconductors can now be plausibly studied using large-scale computer simulations. In general, these simulations fall into two categories: (i) ''first-principles,'' and (ii) ''empirical potential'' methods. First-principles approaches, such as the Car-Parrinello type quantum molecular-dynamics (CPMD),[7] treat both ionic and electronic degrees of freedom in the liquid state in a combined quantum molecular-dynamics calculation. By now, such methods have been used by several groups to calculate the thermophysical properties of liquid semiconductors.[8–13] However, they have the disadvantage of being difficult to apply to large systems — typically, the simulation cell size is not more than several hundred atoms — because of the very time-consuming electronic structure calculations that are required. A semiempirical tight-binding molecular-dynamics (TBMD) method,[14–16] which treats the electronic structure more simply, typically allows a simulation cell as large as several thousand atoms. By contrast, method (ii) describes interatomic interactions in the liquid state using frankly empirical potentials which are fitted to various measured quantities. This approach can usually treat much larger systems and more complex geometries than method (i), but obviously has less grounding in the basics of the electronic structure. The results of these two approaches are therefore complementary.

The present study describes the results of classical molecular-dynamics (MD) simulations as applied to atomic diffusion in liquid Si (ℓ-Si) and liquid Ge (ℓ-Ge) and their alloys. The empirical interatomic potentials are taken as sums of two- and three-body potentials of a form originally suggested by Stillinger and Weber (SW).[17] The MD approach can accurately reproduce the trajectory of the system in phase space, given the potential, and can be performed with millions of atoms, even for SW-type potentials. Hence the applicability of the classical MD method is mostly limited by the realism of the model potentials. Also, for this size of simulation cell, one can study the behavior of even relatively dilute alloys with quite a good statistical resolution.

Of the elemental semiconductors, Si and Ge are commercially the most important. Both are semiconducting in the

TABLE I. SW parameters for Si, model-A Ge, model-B Ge, and ''scaled'' Ge as discussed in the text.

	ε (eV)	σ (Å)	λ
Model Si	2.315	2.095	21.0
Model Ge (A)	1.925	2.181	19.5
Model Ge (B)	1.740	2.215	19.5
''Scaled'' Ge	1.662	2.215	21.0

solid phase, but metallic in the liquid phase. For ℓ-Si, there have already been a number of classical MD studies using the SW potential.[17–21] These yield a good agreement with experimental measurements of the melting temperature T_m, liquid pair distribution functions $g(r)$ and structure factors $S(k)$, liquid density, etc. The calculated velocity autocorrelation functions, however, do differ somewhat from the *ab initio* calculations. ℓ-Ge has been less studied via classical simulations, partly because of the absence of a reliable empirical potential.[22] Among the published work, Hafner and co-workers calculated the liquid structure of Ge, Si, and GaAs using a classical molecular-dynamics method combined with pair potentials and volume-dependent energies derived from pseudopotential theory.[23–25] Wang and Stroud investigated the liquid-vapor interface of several semiconductors, using Monte Carlo simulations and a modified SW potential.[26] The study of impurity diffusion in elemental liquid semiconductors remains unexplored.

The remainder of this paper is organized as follows. Section II describes our calculation model and numerical method for applying it to liquid Si, Ge, and their alloys. Our results are presented in Sec. III, followed by a brief discussion and concluding remarks in Sec. IV.

II. MODEL HAMILTONIAN AND CALCULATIONAL METHOD

A. Empirical interatomic potential

Of the many empirical model potentials which have been developed for Si in various phases,[27] that of Stillinger and Weber[17] has been among the most successful in that it reproduces many properties of both crystalline and liquid Si. It takes the following form:

$$\Phi=\sum_{i<j}\varepsilon f_2(r_{ij}/\sigma)+\sum_{i<j<k}\lambda\varepsilon f_3(\vec{r}_i/\sigma,\vec{r}_j/\sigma,\vec{r}_k/\sigma). \quad (1)$$

Here f_2 is the pair interaction term, f_3 the three-body interaction term which stabilizes the tetrahedral structure of bulk Si, ε the potential well depth, σ is a length parameter, and λ is a scaling factor which reflects the relative strength of the two- and three-body interactions. The values of ε, σ, and λ for Si are shown in Table I. The functional forms and the associated parameter values of f_2 and f_3 can be found in Ref. 17.

Ge has the same crystal structure and very similar thermophysical properties to Si. A SW potential has been parametrized for both crystalline and amorphous Ge,[28,29] but, to our knowledge, no single set of parameters has been found for the SW potential which accurately fits both crystalline and liquid Ge.

In the present calculations, we obtain the Ge parameters by two different methods (to be labeled A and B). In method A, we simply scale the SW values of σ and ε for Si by the appropriate ratios of the Ge/Si lattice constants and cohesive energies, as in Refs. 28 and 29. In addition, we adjust the parameter λ (which measures the relative strengths of the three- and two-body potentials) in such a way that the calculated and measured melting temperatures T_m's are in reasonable agreement. The resulting values of ε, σ, and λ are shown in Table I.

In method B, we scale the SW value of σ such that $\sigma^3 n$ has the same value for *liquid* Si and *liquid* Ge (n being the atomic number density in the liquid state). This choice is motivated by a scaling relation which is proven below. We also reduce the value of the three-body parameter λ slightly from its value in Si, to reflect the somewhat weaker three-body forces expected in ℓ-Ge, and we adjust ε so as to reproduce the observed melting temperature T_m of ℓ-Ge. The resulting values of ε, σ, and λ are also shown in Table I. With this choice, we obtain a structure factor which is in much better agreement with experiments than method A.

We have carried out alloy simulations of liquid Ge containing Si impurities, but only for model A Ge. In this case, for the Ge-Si interactions, we used a SW potential together with the approximations of Karimi *et al.*[30] and of Roland and Gilmer[31]—namely, $\varepsilon_{\text{Si-Ge}}=(\varepsilon_{\text{Si}}\varepsilon_{\text{Ge}})^{1/2}$, $\sigma_{\text{Si-Ge}}=1/2(\sigma_{\text{Si}}+\sigma_{\text{Ge}})$, and $\lambda_{\text{Si-Ge}}=(\lambda_{\text{Si}}\lambda_{\text{Ge}})^{1/2}$.

In all cases, our actual calculations are greatly simplified by decomposing the three-body potential part into products of two-body potentials. With this procedure, direct calculation of the three-body interactions can be avoided, and Newton's third law is applicable in the three-body interaction calculations.[32]

B. Simulation procedure

We carry out our MD simulations within the so-called (N,E,V) ensemble, i.e., the microcanonical ensemble, in which the particle number N, internal energy E, and total volume V are held constant. We use a simple cubic simulation cell with periodic boundary conditions. To integrate the Newtonian equations of motion, we use the velocity Verlet algorithm,[33] with a time step of 0.5 fs. With this approach, E/N is conserved at least within a precision of 10^{-5} eV even at temperatures as high as 2000 K.

Typically, we initialized our simulations with the system in the diamond structure but at the zero-pressure density of the *liquid* state at melting, namely, 2.53 g/cm^3 for Si and 5.53 g/cm^3 for Ge. For Ge containing Si impurities, we initialized a pure Ge simulation cell as described above, then replaced 1/32 of the Ge atoms by Si atom to obtain $\text{Ge}_{0.96875}\text{Si}_{0.03125}$. For pure Si and Ge, our cell contained 4092 atoms, and, for $\text{Ge}_{0.96875}\text{Si}_{0.03125}$, 21 952 atoms, of which 686 were Si atoms. The initial velocities were drawn from a Maxwellian distribution at 500 K. The system total energy was then increased sequentially by about 0.01 eV per atom by velocity rescaling. After each velocity rescaling, 6000 MD steps (3 ps) were run in order to determine whether the system has melted. The system was deemed to start melting when the diffusion coefficient $D(T)$ became larger than 10^{-5} cm^2/s. After the system melted, we ran a total of

12 000 MD steps (6 ps) after each velocity rescaling. In each simulation at a given total energy E, the first 2000 MD steps (1 ps) were discarded for equilibration, and the remainder were used to accumulate statistical averages.

Once the phase-space trajectory of the system has been determined, the atomic pair distribution function $g(r)$ can be calculated using the recipe in Ref. 33. The structure factor $S(k)$, which is related to $g(r)$ by the equation

$$S(k)=1+\frac{4\pi N}{V}\int_0^\infty [g(r)-1]\frac{\sin(kr)}{kr}r^2dr, \tag{2}$$

can also be calculated. Here k is the wave number.

In both pure liquid and liquid alloy, we have calculated the atomic self-diffusion coefficients $D_{\alpha\alpha}$ for atoms of species α, using both the Einstein relation and an appropriate Green-Kubo relation. In the Einstein relation, $D_{\alpha\alpha}$ is determined by

$$D_{\alpha\alpha}=\lim_{t\to\infty}\frac{1}{6t}\langle r^2(t)\rangle_\alpha . \tag{3}$$

The mean-square atomic displacement $\langle r^2(t)\rangle_\alpha$ for atoms of species α is defined as

$$\langle r^2(t)\rangle_\alpha=\frac{1}{N_\alpha}\left\langle \sum_{i=1}^{N_\alpha}\left|\vec{r}_i(t+t_0)-\vec{r}_i(t_0)\right|^2\right\rangle_{t_0} . \tag{4}$$

Here t_0 is an arbitrary initial time, N_α is the number of atoms of species α, $\vec{r}_i(t)$ is the position of the ith atom of species α at time t, and $\langle\ \rangle_{t_0}$ denotes an average over different starting times t_0. In the Green-Kubo approach, $D_{\alpha\alpha}$ is determined from

$$D_{\alpha\alpha}=\frac{1}{3N_\alpha}\sum_{i=1}^{N_\alpha}\int_0^\infty \langle \vec{v}_i(t_0)\cdot\vec{v}_i(t+t_0)\rangle_{t_0}dt, \tag{5}$$

where $\vec{v}_i(t)$ is the velocity of the ith atom of species α at time t.

In most cases we have also fitted the calculated temperature-dependent coefficients $D_{\alpha\alpha}(T)$ to the Arrhenius form

$$D_{\alpha\alpha}(T)=D_0\exp\left(-\frac{E_d}{k_BT}\right), \tag{6}$$

using a least-squares method. Here E_d is the diffusion activation energy, D_0 is the preexponential factor, and T is the temperature. We emphasize that there is no physical reason to expect an activated behavior of the diffusion coefficient in the liquid state; the fit is carried out purely because this form has become customary. The fitting results are actually surprisingly good.

Finally, we calculated the atomic velocity autocorrelation functions

$$Z_{\alpha\alpha}(t)=\sum_{i=1}^{N_\alpha}\langle \vec{v}_i(t_0)\cdot\vec{v}_i(t+t_0)\rangle_{t_0}\Big/\sum_{i=1}^{N_\alpha}\langle \vec{v}_i(t_0)\cdot\vec{v}_i(t_0)\rangle_{t_0}, \tag{7}$$

as well as their power spectra

$$Z_{\alpha\alpha}(\omega)=\int_0^\infty Z_{\alpha\alpha}(t)\cos(\omega t)dt. \tag{8}$$

For notational simplicity, we henceforth drop the subscripts on $D_{\alpha\alpha}(T)$, $Z_{\alpha\alpha}(t)$, $Z_{\alpha\alpha}(\omega)$, and $\langle r^2(t)\rangle_\alpha$ for elemental systems.

C. Scaling of numerical results

Because of the special form of the potential (1), both the static and dynamical properties of the SW liquid satisfy certain simple scaling relations. Since most of these can be derived straightforwardly, we write them down without proof. First, the internal energy E is, in principle, a function of the thermodynamic variables T, V, and N, as well as the parameters σ, ε, and λ. But because of the way in which these parameters appear in the potential, E may be written in the scaling form

$$E=N\varepsilon\mathcal{U}\left(\frac{k_BT}{\varepsilon},\eta,\lambda\right), \tag{9}$$

where

$$\eta=n\sigma^3 \tag{10}$$

is a measure of the effective volume fraction occupied by the interacting atoms. Similarly, the correlation functions $g(r)$ can be expressed as

$$g(r)=\mathcal{G}\left(\frac{r}{\sigma},\frac{k_BT}{\varepsilon},\eta,\lambda\right), \tag{11}$$

while the structure factor $S(k)$ can be written

$$S(k)=\mathcal{S}\left(k\sigma,\frac{k_BT}{\varepsilon},\eta,\lambda\right). \tag{12}$$

To scale the dynamical properties, we note that the natural units of energy and mass for this potential are ε and the atomic mass M, while the natural time unit is

$$\tau_0=\left(\frac{M\sigma^2}{\varepsilon}\right)^{1/2}. \tag{13}$$

Hence the scaling form of the diffusion constant D, which has units of [length]^2/[time], is

$$D=\sigma\left(\frac{\epsilon}{M}\right)^{1/2}\mathcal{D}\left(\frac{k_BT}{\varepsilon},\eta,\lambda\right). \tag{14}$$

Similarly, $Z(t)$ (for a one-component fluid) can be written

$$Z(t)=\mathcal{Z}\left(\frac{t}{\tau_0},\frac{k_BT}{\varepsilon},\eta,\lambda\right), \tag{15}$$

while

$$Z(\omega)=\mathcal{Z}\left(\omega\tau_0,\frac{k_BT}{\varepsilon},\eta,\lambda\right). \tag{16}$$

Similar scaling forms also hold for the Lennard-Jones potential, which is also described by a range parameter σ and strength parameter ε. The main difference is that the SW

potential has an additional dimensionless parameter λ, which simply appears as an extra variable in the scaling functions.

III. NUMERICAL RESULTS

A. ℓ-Si

Since ℓ-Si has been extensively studied using the SW potential, we present our own results mainly as a comparison with previous work. Figure 1 shows the calculated $g(r)$, $S(k)$, $Z(t)$, and $Z(\omega)$ for ℓ-Si at two temperatures. The first two peaks in the calculated $g(r)$ appear at 2.50 and 3.80 Å, in good agreement with experimental values of 2.50 (Refs. 3 and 4) and 3.78 Å.[3] Between these two peaks, our calculated $g(r)$ exhibits a weak peak at 3.23 Å which diminishes with increasing temperature.

The first two peaks of the calculated $S(k)$ [Fig. 1(b)] occur at 2.43 and 5.7 $Å^{-1}$, very close to the experimental values of 2.78 and 5.35 $Å^{-1}$.[3,4] In the experimental $S(k)$, there is a shoulder on the high-k side of the first peak near 3.3 $Å^{-1}$. At the corresponding position in our calculated $S(k)$, the shoulder emerges as a weak secondary peak at 1759 K, which evolves into more of a plateau with increasing temperature. It is thought that this peak is probably a residue of angular (covalent bonding) interactions in liquid Si. As the temperature increases, the covalency effects should become weaker in comparison to two-body central interactions. Such a picture seems to be consistent with the peak-to-plateau transition in our simulations.

Our results for $Z(t)$ and $Z(\omega)$ [Fig. 1(c)] are quite similar to those obtained by TBMD,[14] but differ significantly from the CPMD results.[8,9] In the latter, $Z(t)$ is always positive, so that $Z(\omega)$ monotonically decreases with increasing ω. By contrast, $Z(t)$ from both TBMD and the present calculations oscillate around zero (though they differ somewhat in the peak and trough positions). Our calculated $Z(t)$ has an oscillation period of about 0.064 ps. The corresponding $Z(\omega)$ at 1759 K shows two peaks at $\hbar\omega = 11$ and 57 meV. At 1970 K, the first peak weakens and shifts to 9 meV, while the second changes little. The TBMD $Z(\omega)$ exhibits only a single peak, which appears at a frequency close to our calculated second peak. Ishimaru, Yoshida, and Motooka[21] also calculated $Z(t)$, using the same empirical potential and integration method as ours. Their first peak, however, is distinctly negative, in contrast to ours. We tentatively attribute these differences to the large MD time step (2 fs) in their simulations, which may not be sufficiently small to allow for accurate integration of the Newtonian equations.

Figure 2 displays the self-diffusion coefficients $D(T)$ of liquid Si as obtained from the Einstein relation (□ points), and from the Green-Kubo-type integration of the velocity autocorrelation functions (+ points). Evidently, $\ln D(T)$ behaves in a reasonably linear fashion with $1/T$, suggesting an activated Arrhenius-type behavior, as in Eq. (6). Table II shows the Arrhenius parameters as obtained from a least-squares fit. E and K in the table denote that $D_{\alpha\alpha}(T)$ is calculated from the Einstein relation and from the Green-Kubo-like integration of $Z_{\alpha\alpha}(t)$, respectively. The Einstein and Green-Kubo activation energies E_d agree to within about 0.05 eV. There appears to be no reliable experimental numbers with which to compare these results. We emphasize,

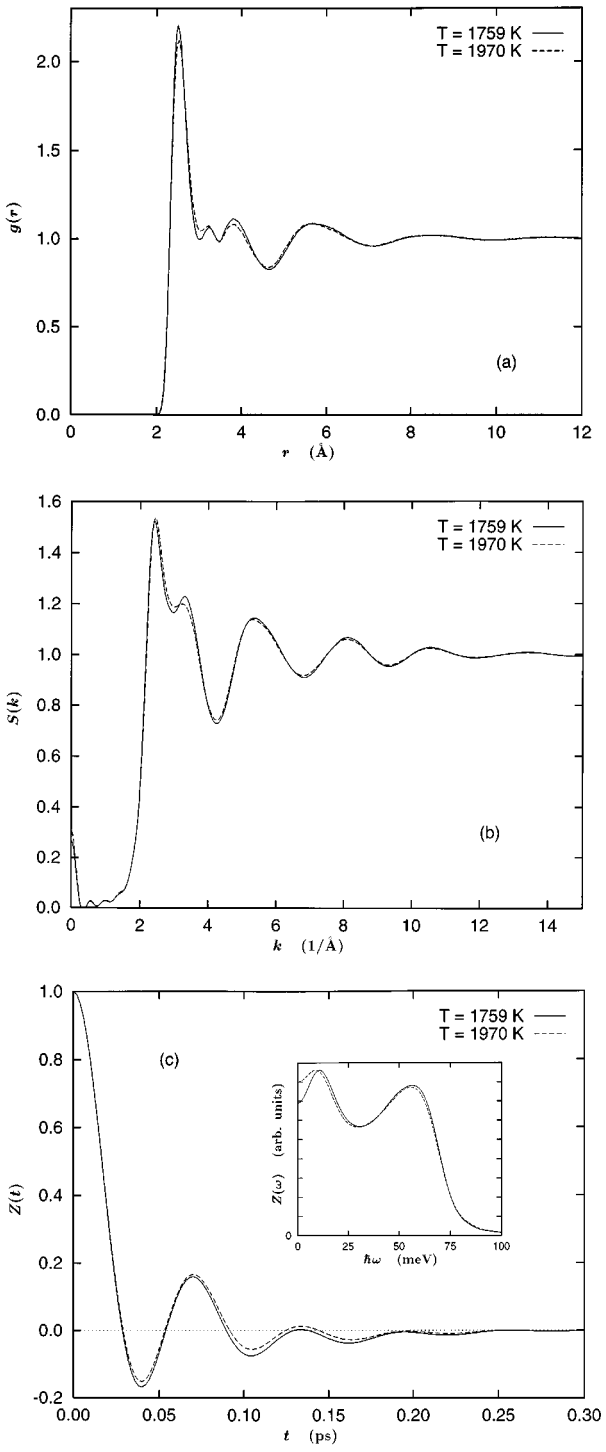

FIG. 1. Calculated (a) pair distribution function $g(r)$, (b) liquid structure factor $S(k)$, and (c) velocity autocorrelation function $Z(t)$ and its power spectrum $Z(\omega)$ (inset), for ℓ-Si.

however, that these Arrhenius fits are obtained over a relatively limited range of temperatures and diffusion coefficients, and many other functional forms, such as $D(T) = aT + b$, would have given fits of nearly equal quality to the Arrhenius one.

Our calculated values of E_d are larger than the value 0.27 eV quoted by Kakimoto.[20] His calculations, however, are based on a modified SW potential[29] with much smaller λ

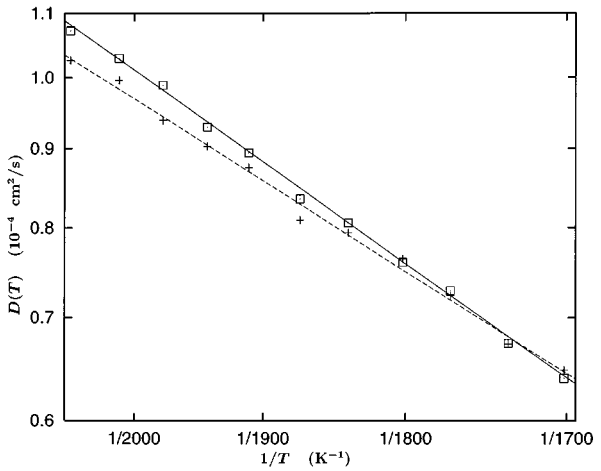

FIG. 2. Calculated self-diffusion coefficient $D(T)$ for ℓ-Si, plotted semilogarithmically vs inverse temperature $1/T$. □, results from the Einstein relation; +, from an integration of $Z(t)$. Full and dashed straight lines are the results of least-squares fits of the simulation data to the Arrhenius expression $D(T)=D_0\exp(-E_d/k_BT)$; the fitted D_0 and E_d are shown in Table II.

than the original. The measured shear viscosity $\nu(T)$ is also sometimes fitted to Arrhenius form.[34] The value of E_d based on the measured $\nu(T)$ is about 0.37 eV, which agrees quite well with our results.

Finally, we briefly compare our numerical results to other studies. Our values for $D(T)$ (about 6.39×10^{-5} cm^2/s at 1700 K) are close to previous SW simulations[18] [carried out in the (N,T,P) ensemble] but smaller than either the *ab initio* results of about 2.0×10^{-4} cm^2/s at 1800 K,[8,9] or the tight-binding values of 1.1 to 1.7×10^{-4} cm^2/s at 1780 K.[14–16] The reasons for these differences are not known.

B. "Scaled" ℓ-Ge

There is a strong similarity between the structure factors of liquid Si and Ge near their melting points. Both have a principal peak which reaches a maximum of only about 1.7, compared to the value of 2.5–2.8 more typical of close-packed liquid metals near their melting point. More strikingly, both have a conspicuous shoulder on the large-k side of the first peak. While this shoulder is slightly more conspicuous in ℓ-Si than in ℓ-Ge, the structure factors, to a good approximation, are simply scaled versions of one another. This fact suggests the use of a scaled SW potential for ℓ-Ge. That is, we initially scale ε by the ratio of the melting temperature T_m, and σ by a factor such that $n_{\rm Ge}\sigma_{\rm Ge}^3=n_{\rm Si}\sigma_{\rm Si}^3$, where $n_{\rm Ge}$ and $n_{\rm Si}$ are the number densities of liquid Ge and Si at melting. In order to obtain a truly scaled liquid, we retain the same value of λ, although one might expect a slightly smaller value of λ for ℓ-Ge than for ℓ-Si, in order to reproduce the slightly weaker shoulder. The values of the parameters for "scaled" ℓ-Ge are shown in Table I.

TABLE II. Self-diffusion activation energies E_d and preexponential factors D_0 obtained by least-squares fits of the simulation results to the Arrhenius form. In the calculation method, E and K denote that $D(T)_{\alpha\alpha}$ is calculated from the Einstein relation and from the Green-Kubo-like integration of $Z_{\alpha\alpha}(t)$, respectively.

System	Atom type	Calc. method	D_0 ($\times10^{-4}$ cm^2/s)	E_d (eV)
ℓ-Si		E	13.53	0.447
		K	9.82	0.399
ℓ-Ge (A)	Ge	E	6.69	0.332
		K	5.30	0.295
	Ge	E	7.91	0.358
ℓ-Ge (A) with		K	5.63	0.311
Si Impurity	Si	E	9.80	0.385
		K	6.95	0.339
ℓ-Ge (B)	Ge	E	4.98	0.262
		K	4.54	0.253

The temperature-dependent diffusion coefficient of scaled Ge, $D_{\rm Ge}(T)$, can immediately be written down in terms of $D_{\rm Si}(T)$, the diffusion coefficient of Si, using Eq. (14). The result is

$$D_{\rm Ge}(T)=\frac{\sigma_{\rm Ge}}{\sigma_{\rm Si}}\left(\frac{\varepsilon_{\rm Ge}}{\varepsilon_{\rm Si}}\right)^{1/2}\left(\frac{M_{\rm Si}}{M_{\rm Ge}}\right)^{1/2}D_{\rm Si}(T'), \tag{17}$$

where

$$\frac{T}{T_m^{\rm Ge}}=\frac{T'}{T_m^{\rm Si}}, \tag{18}$$

$T_m^{\rm Ge}=1211$ K and $T_m^{\rm Si}=1687$ K being the melting temperatures of Ge and Si at ordinary pressure.[35] If we substitute the parameter values given in Table I and $D_{\rm Si}(T_m^{\rm Si})$ from our simulations, we obtain

$$D_{\rm Ge}(T_m^{\rm Ge})\approx0.56D_{\rm Si}(T_m^{\rm Si})\approx3.6\times10^{-5}\ {\rm cm}^2/{\rm s}. \tag{19}$$

From Eq. (17), the Arrhenius coefficients of scaled Ge are

$$D_0^{\rm Ge}=\frac{\sigma_{\rm Ge}}{\sigma_{\rm Si}}\left(\frac{\varepsilon_{\rm Ge}}{\varepsilon_{\rm Si}}\right)^{1/2}\left(\frac{M_{\rm Si}}{M_{\rm Ge}}\right)^{1/2}D_0^{\rm Si}\approx0.56D_0^{\rm Si} \tag{20}$$

and

$$E_d^{\rm Ge}=\frac{T_m^{\rm Ge}}{T_m^{\rm Si}}E_d^{\rm Si}\approx0.72E_d^{\rm Si}. \tag{21}$$

C. ℓ-Ge: Model A

Figure 3 shows the calculated mean potential energy per atom $\langle\Phi(T)/N\rangle$ for Ge, as obtained from (N,E,V) MD simulations and the model-A SW potential for Ge parametrized in Table I. As in Si,[17] the S-shaped curve characterizes a first-order solid-liquid phase transition. As is well known, it is difficult to obtain a reliable thermodynamical potential melting temperature from (N,E,V) MD simulations, especially when the system exhibits a first-order phase transition at melting. As energy is added to the crystalline system, there is first a "superheated" region, just as in real superheated crystals. At the end of this superheating region, the system enters a thermodynamically unstable "retrograde" regime, where the system starts to melt and the temperature actually decreases during melting even though E

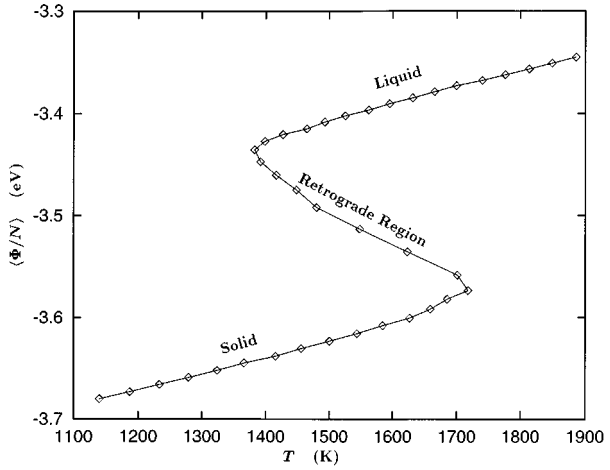

FIG. 3. Average potential energy per atom, $\langle \Phi/N \rangle$, plotted vs T for model-A Ge, as obtained from (N,E,V) MD simulations. The line is a guide to the eye.

increases. The functional form of $\langle \Phi(T)/N \rangle$ in this retrograde region, as well as the limits of this region, both depend on the length and heating rate of the MD simulations. If the heating rate is slow enough and the MD simulations run long enough, the low-temperature end of the retrograde region can usually give a good approximation of the potential thermodynamical melting point. In our Si simulations, the retrograde region ends at $\sim$1700 K, which is just 7 K higher than the potential melting temperature calculated by Broughton and Li.[18] For our model-A Ge, the retrograde region ends at $\sim$1382 K, about 160 K above the experimentally observed Ge melting temperature T_m^{Ge}. Following the retrograde region, the system enters the normal liquid state, where T increases with increasing E. Such behavior is similar to expectations in real supercooling and superheating experiments. All our calculated ℓ-Ge properties are obtained in the normal liquid region.

The corresponding liquid $g(r)$ and $S(k)$ are shown in Figs. 4(a) and 4(b). The principal peak in $g(r)$ occurs near $r=2.65$ Å, in good agreement with the values of 2.82 Å at 1253 K by x-ray diffraction,[3] and of 2.63 Å (1233 K) and 2.67 Å (1573 K) by neutron diffraction.[4] The second peak occurs at 4.10 Å, in good agreement with the observed 4.21 Å.[3] The calculated $S(k)$ agrees well with experiments except in the first peak, which in experiments has a weak high-k shoulder. In our model-A calculations, this ''shoulder'' is actually slightly stronger than the first peak, although both fall in the correct positions. With increasing T, in our calculations, the shoulder and peak merge into a single stronger principal peak. The model-B calculations below give a value of $S(k)$ in better agreement with experiments.

The calculated model-A $Z(t)$ and $Z(\omega)$ for ℓ-Ge [Fig. 4(c)] closely resemble those of ℓ-Si, but differ from the *ab initio* results for both ℓ-Ge (Refs. 10 and 11) and ℓ-Si.[8,9] For ℓ-Ge, our calculated $Z(t)$ has an oscillation period of about 0.12 ps, about twice that of ℓ-Si.

In Fig. 5, we plot $D(T)$ for model A ℓ-Ge, as obtained both from the Einstein relation method ($\square$ points) and from an integration of $Z(t)$ ($+$ points). The linear dependence of

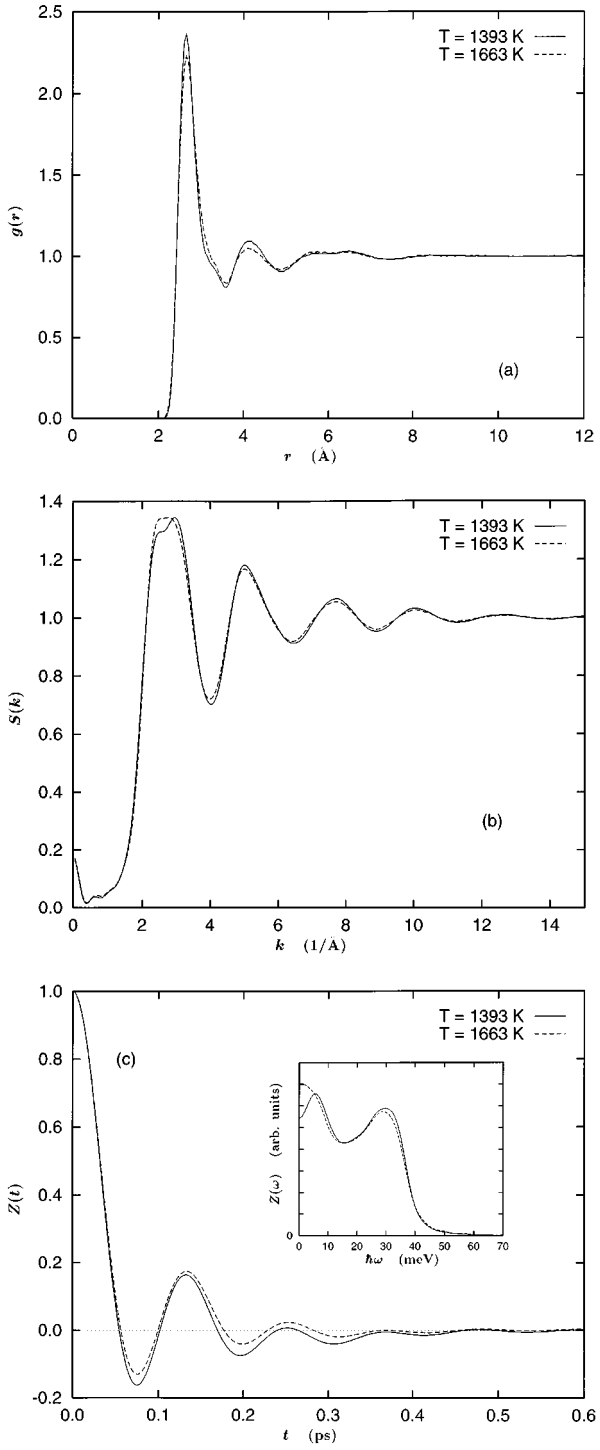

FIG. 4. Same as Fig. 1, but for model-A ℓ-Ge.

$\ln D(T)$ on $1/T$ suggests an Arrhenius relation, Eq. (6). The diffusion activation energy E_d and preexponential factor D_0, as obtained from a least-squares fit, are shown in Table II; both agree to within 0.04 eV.

Our calculated $D(T)$ is substantially smaller than *ab initio* values of 1.0×10^{-4} cm^2/s at 1230,[10,11] and 1.4×10^{-4} cm^2/s at 1400 K.[13] They are also smaller than quoted experimental values,[1] which may be influenced by convective forces.

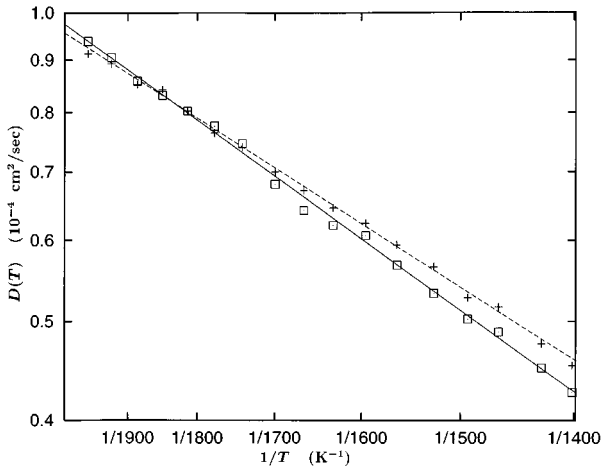

FIG. 5. Same as Fig. 2, but for model-A ℓ-Ge.

D. Model-A ℓ-Ge containing Si impurities

Figure 6 shows the calculated $D_{\alpha\alpha}(T)$ for Ge and Si atoms in liquid $Ge_{0.96875}Si_{0.03125}$, as calculated from the Einstein relation, and from $Z_{\alpha\alpha}(t)$, using model-A potentials for ℓ-Ge. The calculated Arrhenius parameters are shown in Table II. Evidently, both diffusion coefficients are quite similar; presumably, the larger masses of the Ge atoms is compensated for by the slightly weaker interionic forces, so that the resulting diffusion coefficients are not very different.

Figure 7 shows the corresponding $Z_{\alpha\alpha}(t)$ and $Z_{\alpha\alpha}(\omega)$, as well as the mean-square atomic displacements $\langle r^2(t)\rangle_\alpha$ for the same alloy. The linear dependency of $\langle r^2(t)\rangle_\alpha$ of both species on time t characterizes clear diffusive atomic motions, as is expected in liquid state. The oscillation frequencies of the $Z_{\alpha\alpha}(t)$'s are different, presumably reflecting mainly the differences in atomic masses.

E. ℓ-Ge: Model B

We also carried out simulations on a slight modification of ''scaled'' ℓ-Ge. Specifically, we reduce λ from 21.0 to 19.5 to reflect the expected slightly weaker three-body forces; and we increase ε slightly to give a more accurate T_m^{Ge}. The resulting $g(r)$ and $S(k)$ are shown in Fig. 8. As expected, the high-k shoulder on the first peak of $S(k)$ is weakened by reducing λ. This agrees with experiments on ℓ-Ge,[3,4] which show a weaker shoulder than for ℓ-Si. Indeed, with these parameters, the entire structure factor of ℓ-Ge agrees well with experiments, in both the first and higher peaks. We also calculated $Z(t)$ and $Z(\omega)$ for these potentials; they are very similar to that of model A.

Figure 9 shows $D(T)$ for these parameters. It behaves very similarly to that of model A. Once again, it is substantially smaller than the *ab initio* results and available experiments. The fitted Arrhenius E_d and D_0 for the model-B potential are also shown in Table II.

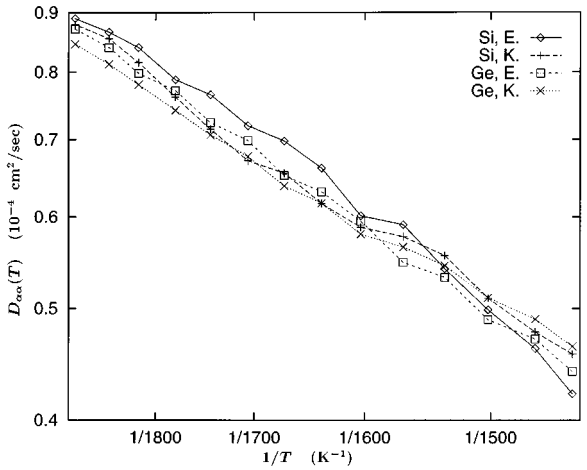

FIG. 6. Calculated $D_{\alpha\alpha}(T)$'s for model-A liquid $Ge_{0.96875}Si_{0.03125}$. In the legend, Si and Ge refer to the atom types, E and K denote that $D(T)_{\alpha\alpha}$ is calculated from the Einstein relation and from the Green-Kubo-like integration of $Z_{\alpha\alpha}(t)$, respectively.

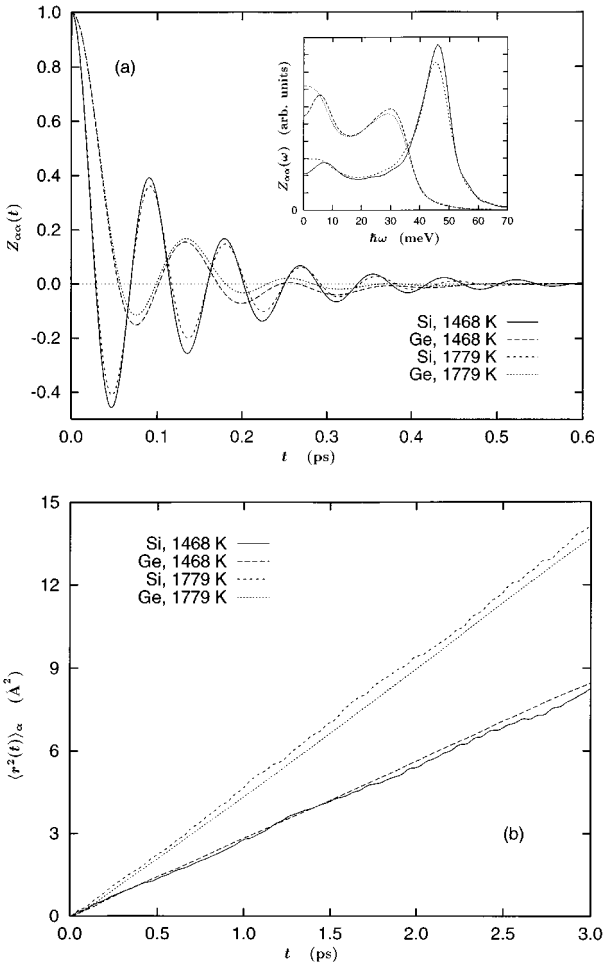

FIG. 7. Calculated (a) velocity autocorrelation functions $Z_{\alpha\alpha}(t)$ and its power spectra $Z_{\alpha\alpha}(\omega)$ (inset), and (b) atomic mean-square displacement $\langle r^2(t)\rangle_\alpha$, for liquid model-A $Ge_{0.96875}Si_{0.03125}$, at two temperatures.

IV. DISCUSSION AND SUMMARY

We have presented extensive numerical studies of both the static and dynamical properties of ℓ-Si and ℓ-Ge, using the SW model potential in conjunction with classical MD in the (N,E,V) ensemble. We use a very efficient numerical algorithm in which the three-body part of the SW potential is

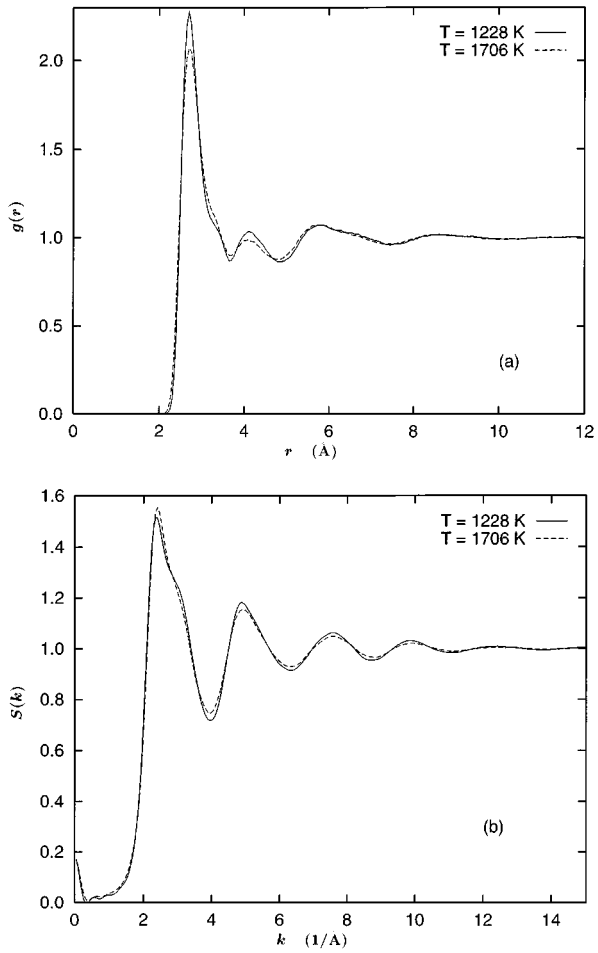

FIG. 8. Calculated (a) $g(r)$ and (b) $S(k)$ for model-B ℓ-Ge at two temperatures.

split into products of two-body potentials. To optimize the agreement of the calculated $S(k)$'s with experiments, we considered two different ways of choosing the SW parameters for ℓ-Ge. Both yield $S(k)$'s for both ℓ-Si and ℓ-Ge in generally good agreement with experiments, including a conspicuous shoulder on the first peak. But one choice, in which the SW parameter σ is scaled by the cubic root of the liquid atom density, agrees better for the *strength* of that shoulder, which is weaker than the corresponding shoulder in ℓ-Si. We find that the calculated $S(k)$ is consistent with the intuitive expectation that three-body forces in ℓ-Ge are slightly weaker than in ℓ-Si, based on the fact that Ge is a heavier atom and has a smaller band gap in the solid phase. The values of the parameters seem to be somewhat different than those which fit the behavior of *amorphous* Ge.[28]

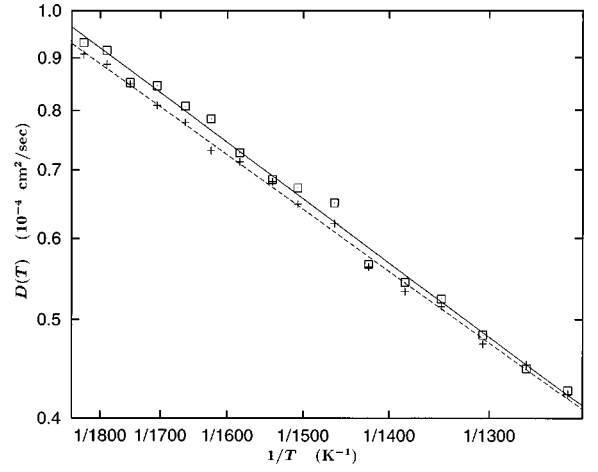

FIG. 9. Same as Fig. 2, but for model-B ℓ-Ge.

We find that, in all cases, our calculated diffusion coefficients can be fitted reasonably well to an Arrhenius form. Although this is a useful analytical form, other analytical forms [such as a simple straight-line temperature dependence $D(T)=a+bT$] would probably fit the data equally well; in any event there is no underlying physical reason to expect an activated form for the diffusion coefficient of a classical liquid. Thus we do not ascribe a great physical significance to this fit.

The calculated self-diffusion coefficients for both ℓ-Si and ℓ-Ge are at least a factor of 2 smaller than reported *ab initio* results, as well as quoted experimental values. This should probably not be given great significance at present, because the experimental results are all obtained in ambient gravity. They are therefore likely to be strongly affected by convection, which should give a spuriously large value of the diffusion coefficient. Nevertheless, there are several possible reasons why the present calculations may give low values of $D(T)$ for ℓ-Si and ℓ-Ge. Most importantly, the present calculations describe the entire potential energy of (metallic) ℓ-Si and ℓ-Ge as a sum of two and three-body potentials. Since simple metals are known to have a large volume-dependent, structure-independent term in their energy, this description is clearly oversimplified. It is not obvious, however, just how this simplification would affect the calculated diffusion coefficients; thus the error made in the SW decomposition remains unknown.

We also carried out a limited number of diffusion calculations for a model of the alloy system $Ge_{0.96875}Si_{0.03125}$. The results indicate that the self-diffusion coefficients of each component are similar, the influence of the smaller ionic mass of the impurity being counterbalanced by the stronger interatomic interactions it experiences. We believe that this qualitative result may be robust; that is, it may be valid beyond the empirical potential approach we use to derive it.

In conclusion, our results show that the SW potential is a useful model for ℓ-Ge as well as ℓ-Si. While its predictions may not be quantitatively accurate for all properties, this potential can be used on a very large scale. This fact may make it applicable to many problems of practical importance involving liquid Ge and Si, including atomic transport properties of mixtures, behavior of liquids in narrow channels, and the properties of liquid-vapor and liquid-solid interfaces.

ACKNOWLEDGMENTS

One of the authors (W. Y.) gratefully acknowledges support provided by Professor Anupam Madhukar through the U.S. Office of Naval Research and thanks Professor Madhukar for a critical reading of the manuscript. Z. Q. W. and D. S. are grateful for support from NASA through Grant No. NAG3-1437. We also acknowledge many useful conversations with D. Matthiesen, A. Chait, R. Kulkarni, and W. Aulbur.

*Present address: WL/MLPJ, Materials Directorate, Air Force Wright Laboratory, WPAFB, OH 45433.

[1] P. V. Pavlov and E. V. Dobrokhotov, Fiz. Tverd. Tela (Leningrad) **12**, 281 (1970) [Sov. Phys. Solid State **12**, 225 (1970)].
[2] K. M. Shvarev, B. A. Baum, and P. V. Gel'd, Fiz. Tverd. Tela (Leningrad) **16**, 3246 (1974) [Sov. Phys. Solid State **16**, 2111 (1975)].
[3] Y. Waseda and K. Suzuki, Z. Phys. B **20**, 339 (1975).
[4] J. P. Gabathuler and S. Steeb, Z. Naturforsch. **34a**, 1314 (1979).
[5] C. F. Hague, C. Sénémaud, and H. Ostrowiecki, J. Phys. F **10**, L267 (1980).
[6] H. Sasaki, E. Tokizaki, K. Terashima, and S. Kimura, J. Cryst. Growth **139**, 225 (1994).
[7] R. Car and M. Parrinello, Phys. Rev. Lett. **55**, 2471 (1985).
[8] I. Štich, R. Car, and M. Parrinello, Phys. Rev. Lett. **63**, 2240 (1989); Phys. Rev. B **44**, 4262 (1991).
[9] J. R. Chelikowsky, N. Troullier, and N. Binggeli, Phys. Rev. B **49**, 114 (1994).
[10] G. Kresse and J. Hafner, Phys. Rev. B **49**, 14 251 (1994).
[11] N. Takeuchi and I. L. Garzón, Phys. Rev. B **50**, 8342 (1994).
[12] O. Sugino and R. Car, Phys. Rev. Lett. **74**, 1823 (1995).
[13] R. V. Kulkarni, W. G. Aulbur, and D. Stroud (unpublished).
[14] R. Virkkunen, K. Laasonen, and R. M. Nieminen, J. Phys. Condens. Matter **3**, 7455 (1991).
[15] C. Z. Wang, C. T. Chan, and K. M. Ho, Phys. Rev. B **45**, 12 227 (1992).
[16] G. Servalli and L. Colombo, Europhys. Lett. **22**, 107 (1993).
[17] F. H. Stillinger and T. A. Weber, Phys. Rev. B **31**, 5262 (1985).
[18] J. Q. Broughton and X. P. Li, Phys. Rev. B **35**, 9120 (1987).
[19] U. Landman, W. D. Luedtke, M. W. Ribarsky, R. N. Barnett, and C. L. Cleveland, Phys. Rev. B **37**, 4637 (1988); W. D. Luedtke, U. Landman, M. W. Ribarsky, R. N. Barnett, and C. L. Cleveland, *ibid.* **37**, 4647 (1988).
[20] K. Kakimoto, J. Appl. Phys. **77**, 4122 (1995).
[21] M. Ishimaru, K. Yoshida, and T. Motooka, Phys. Rev. B **53**, 7176 (1996).
[22] S. J. Cook and P. Clancy, Phys. Rev. B **47**, 7686 (1993).
[23] A. Arnold, N. Mauser, and J. Hafner, J. Phys. Condens. Matter **1**, 965 (1989).
[24] W. Jank and J. Hafner, Phys. Rev. B **41**, 1497 (1990).
[25] W. Jank and J. Hafner, J. Phys. Condens. Matter **1**, 4235 (1989).
[26] Z. Q. Wang and D. Stroud, Phys. Rev. B **38**, 1384 (1988).
[27] For a recent review, see, e.g., H. Balamane, T. Halicioglu, and W. A. Tiller, Phys. Rev. B **46**, 2250 (1992), and references cited therein.
[28] K. Ding and C. Andersen, Phys. Rev. B **34**, 6987 (1986).
[29] J. Zi, K. Zhang, and X. Xie, Phys. Rev. B **41**, 12 915 (1990).
[30] M. Karimi, T. Kaplan, M. Mostoller, and D. E. Jesson, Phys. Rev. B **47**, 9931 (1993).
[31] C. Roland and G. H. Gilmer, Phys. Rev. B **47**, 16 286 (1993).
[32] A. Nakano, P. Vashishta, and R. K. Kalia, Comput. Phys. Commun. **77**, 303 (1993).
[33] M. P. Allen and D. J. Tildesley, *Computer Simulation of Liquids* (Clarendon, Oxford, 1987).
[34] V. M. Glazov, S. N. Chizhevskaya, and N. N. Glagoleva, *Liquid Semiconductors* (Plenum, New York, 1969).
[35] C. Kittel, *Introduction to Solid State Physics*, 6th ed. (Wiley, New York, 1986).